Hearing Research, 39 (1989) 143–158
Elsevier

HRR 01201

Spectral characteristics of the responses of primary auditory-nerve fibers to amplitude-modulated signals

S.M. Khanna and M.C. Teich

Fowler Memorial Laboratory, Department of Otolaryngology, Columbia College of Physicians and Surgeons, New York, New York, U.S.A. and Department of Electrical Engineering, Columbia University, New York, New York, U.S.A.

(Received 11 May 1988; accepted 13 December 1988)

The spectral responses of cat single primary auditory nerve fibers to sinusoidal amplitude-modulated (AM) and double-sideband (DSB) acoustic signals applied to the ear were examined. DSB is an amplitude-modulated signal with a suppressed carrier. Period histograms were compiled from the neural spike-train data, and the frequency spectrum was determined by Fourier transforming these histograms. For DSB signals, spectral components were found to be present at the frequencies of the stimulus as well as at certain combination frequencies. For AM signals, several clusters of spectral components were present. The lowest-frequency cluster consisted of components at DC, at the modulation frequency, and at its harmonics. A higher frequency cluster occurs around a component with the frequency of the carrier. The components of cluster are separated from the carrier by the modulation frequency and its harmonics. Yet higher-frequency clusters appear around multiples of the carrier frequency with components at frequencies separated from these multiples by the modulation frequency and its harmonics. The magnitudes of these spectral components were determined for carrier frequencies located below, at, and above the characteristic frequency of the units, and for different stimulus levels, modulation frequencies, and modulation depths. The low-frequency components present in the neural spike train appear to be the result of demodulation taking place in the inner ear. The demodulated components are strong and are present over a wide range of sound levels, carrier frequencies, modulation frequencies, and nerve-fiber characteristics. This demodulation may be significant for speech recognition.

Auditory-nerve fiber; Amplitude modulation; Neural coding; Spectral characteristics

Introduction

Animals communicate with sounds whose intensities and frequencies vary with time. In human speech, the vocal cords (with the aid of the cavities and orifices of the pharynx, mouth and nose) produce sounds that are both amplitude- and frequency-modulated (Fletcher, 1953). Amplitude modulation (AM) and frequency modulation (FM) are therefore fundamental elements of communication sounds. It is for this reason that the responses to amplitude- and frequency-modulated tones, and other complex time-varying signals, have been studied extensively at many levels of the auditory system, mostly at the cochlear nucleus and at higher levels (Britt and Starr, 1976; de Ribaupierre et al., 1970; Evans and Nelson, 1966; Evans, 1978; Fernald and Gerstein, 1972; Glattke, 1969; Greenwood, 1986, 1988; Horst et al., 1985, 1986; Javel, 1980; Møller, 1971, 1972a, 1972b, 1973, 1974, 1976; Nelson et al., 1966; Sinex and Geisler, 1981; Smith and Brachman, 1980; Vartanian, 1971).

However, Evans (1978), Javel (1980), and Smith and Brachman (1980) studied certain aspects of the responses to AM tones of single primary auditory nerve fibers in the cat, in the chinchilla, and in the Mongolian gerbil, respectively. Javel (1980) compiled period histograms locked to various frequencies associated with the stimulus. He used these histograms to examine the synchronization of the spike discharges to the envelope of the AM wave, and studied the spectral components of the

Correspondence to: S.M. Khanna, Fowler Memorial Laboratory, Department of Otolaryngology, Columbia College of Physicians and Surgeons, New York, N.Y. 10032, U.S.A.

discharge pattern by Fourier transforming those histograms locked to the carrier frequency, or to its lower- and upper-sidebands. He determined the magnitudes of the spectral components as a function of stimulus level, modulation frequency, and modulation depth. Javel showed that the discharge is synchronized to the modulation envelope. Smith and Brachman (1980) studied this feature of the fiber response in terms of the Fourier components of a period histogram that was locked to the modulation frequency. Their study was concerned with the relationship between the spectral component at the modulation frequency as a function of stimulus level, for a range of modulation frequencies and modulation depths with the carrier frequency set to characteristic frequency (CF) of the unit.

In this paper we examine the spectral properties of the response of cat single primary auditory nerve fibers to sinusoidal AM and double-sideband (DSB) acoustic signals. Our analysis is based on period histograms locked to both the modulation frequency and the carrier frequency of the stimulus sound.

Theory

Double-sideband (DSB) signals

The simplest stimulus consisting of more than a single tone is a pair of pure tones of equal magnitude. Two-tone stimuli have been used extensively in studies of eighth-nerve firing patterns (Galambos and Davis, 1944; Sachs and Kiang, 1968;

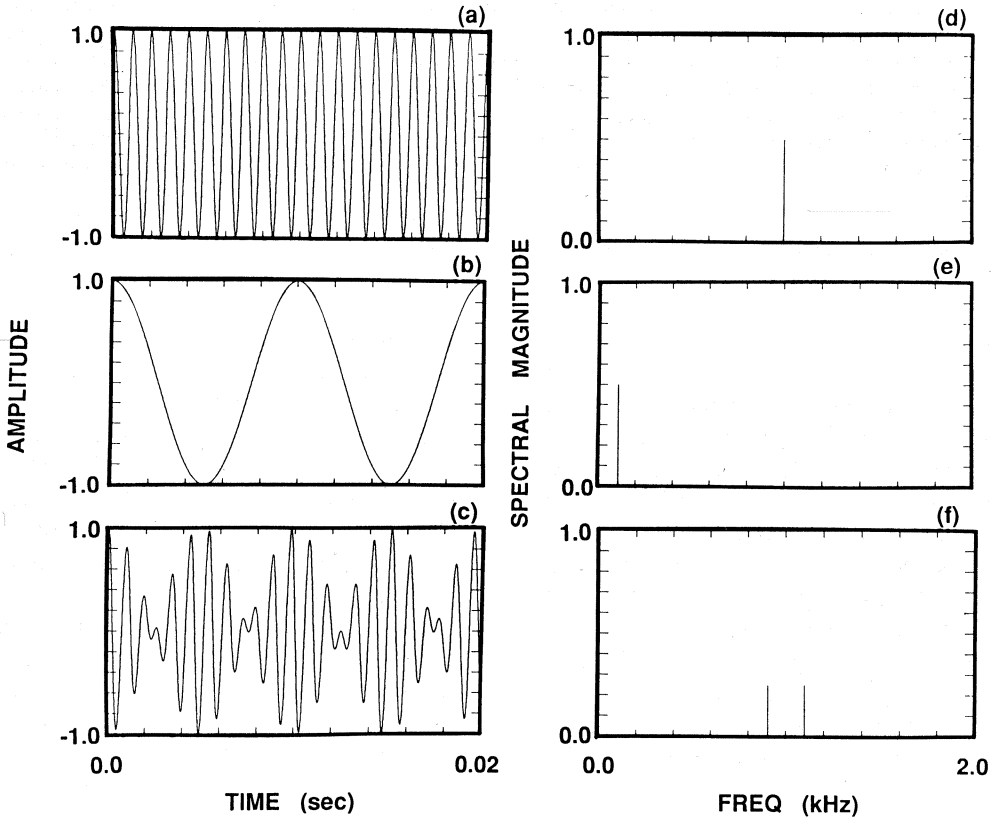

Fig.1. Time course [(a) and (b)] and spectrum [(d) and (e)] of two cosine waves that are multiplied to produce a DSB wave [(c) and (f)]. The modulating wave in (a) has $f_m = 98$ Hz whereas the carrier wave in (b) has $f_c = 996$ Hz. The spectrum of the DSB signal consists of a lower-sideband at $f_1 = f_c - f_m = 898$ Hz and an upper-sideband at $f_2 = f_c + f_m = 1094$ Hz. There is no spectral component at the carrier frequency. Note that for each cycle of the modulating tone, the DSB signal exhibits two wavepackets.

Rose et al., 1968; Arthur et al., 1971; Littlefield, 1973; Abbas and Sachs, 1976; Javel et al., 1978; Javel, 1981; Greenberg et al., 1986).

Our interest in two-tone signals stems from their kinship with AM signals; when the two tones are phase-locked and of equal amplitude, their spectrum is similar to that of an AM signal; the key distinction is that the carrier is suppressed in DSB. For this reason, two-tone stimuli are referred to in the engineering literature as double-sideband suppressed-carrier signals (Schwartz, 1980).

The DSB signal is simply the product of two sinusoidal time waves (Schwartz, 1980). The lower-frequency (modulating) wave is denoted f_m and the higher-frequency (carrier) wave is denoted f_c. The individual time behavior of the sine waves, and their product, are illustrated in Figs. 1 (a)–(c). The spectrum of each of the individual waves consists of a single frequency, as shown in Figs. 1(d) and 1(e). Only positive frequencies are illustrated in the figure since the spectrum is symmetric about zero frequency. The magnitudes of all components are therefore one-half the amplitude of the wave. This convention is followed throughout this paper (Schwartz, 1980).

The spectrum of the DSB signal, illustrated in Fig. 1(f), consists of a lower-sideband (LSB) at frequency $f_1 = f_c - f_m$ and an upper-sideband (USB) of the same amplitude at frequency $f_2 = f_c + f_m$. For the purposes of illustration, f_m and f_c have been taken to be 98 Hz and 996 Hz, respec-

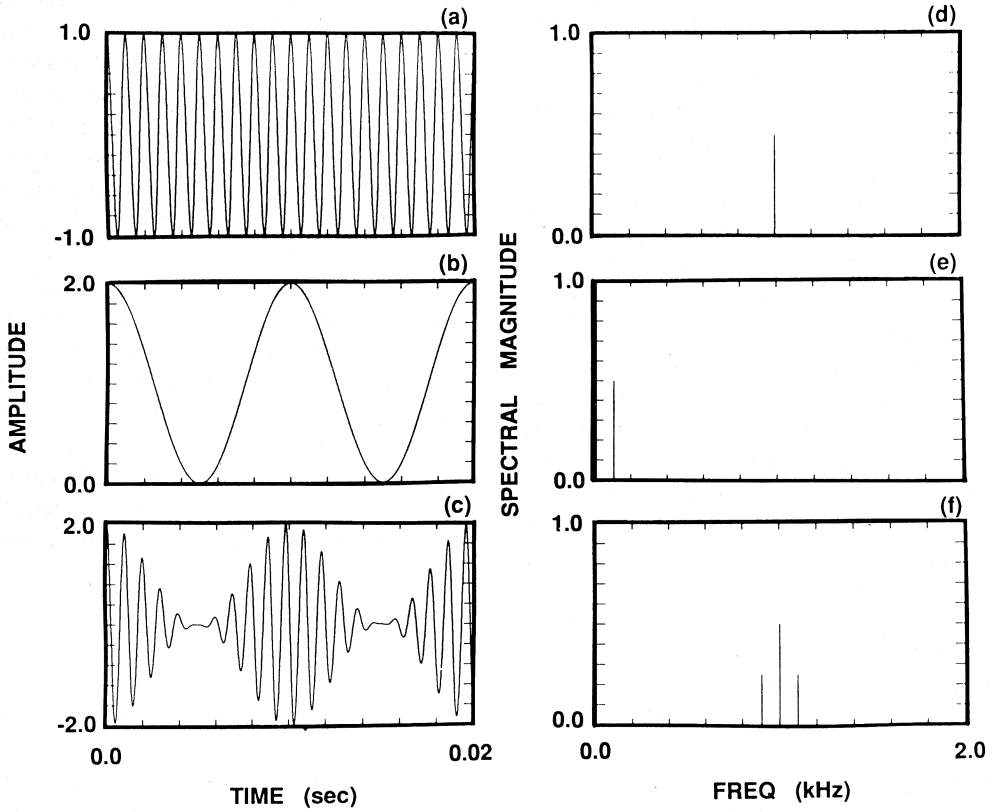

Fig.2. Time course [(a) and (b)] and spectrum [(d) and (e)] of two cosine waves that are used to produce an AM wave with $M = 1$ [(c) and (f)]. The carrier wave in (a) has $f_c = 996$ Hz whereas the modulating wave in (b) has $f_m = 98$ Hz. The spectrum of the AM signal consists of a carrier component at $f_c = 996$ Hz, along with a lower-sideband at $f_c - f_m = 898$ Hz and an upper-sideband at $f_c + f_m = 1094$ Hz, symmetrically placed about the carrier. For 100% modulation depth, the magnitudes of the lower- and upper-sidebands are precisely one-half that of the carrier. Note that for each cycle of the modulating tone the AM signal exhibits only a single wavepacket, in contrast to the two wavepackets exhibited for DSB.

tively, so that $f_1 = 898$ Hz and $f_2 = 1094$ Hz. Thus, the LSB and USB frequencies are 898 Hz and 1094 Hz, respectively. The envelope of the DSB signal depicted in Fig. 1(c) varies at the difference frequency $f_2 - f_1 = 2f_m = 196$ Hz.

Amplitude-modulated (AM) signals

Amplitude modulation is achieved by modulating a sinusoidal wave (the carrier) with another wave of lower frequency (the modulating signal). In general, the modulating signal may be a complex wave as long as its bandwidth is less than half the carrier frequency (Cuccia, 1952). In the simple case considered here, the modulating signal is a cosine wave. In this case the AM signal may be written as

$$s_{AM}(t) = A(1 + M\cos 2\pi f_m t)\cos(2\pi f_c t + \phi) \quad (1)$$

where A is the amplitude of the carrier, f_c is the carrier frequency, f_m is the modulation frequency, and ϕ is its phase. The quantity M represents the depth of modulation ($0\% \leqslant M \leqslant 100\%$). The individual waves, and the modulated wave (Eq. (1) with $M = 1$), are illustrated in Figs. 2(a)–(c), when $f_c = 996$ Hz and $f_m = 98$ Hz. The spectrum of the carrier, the modulation signal, and the modulated signal are illustrated in Figs. 2(d), 2(e), and 2(f), respectively.

The spectrum of the AM signal illustrated in Fig. 2(f) consists of three frequency components, the carrier and the two sidebands separated from the carrier by $\pm$ the modulation frequency. These components are called sidebands because when the modulating wave is complex, bands of spectral components appear below and above the carrier frequency. Thus, compared to DSB, there is an additional component at the carrier frequency f_c. The magnitude of the sidebands is lower than that of the carrier by the factor $M/2$. For $M = 1$ (100% modulation), the sidebands have half the amplitude of the carrier. For the illustration in Fig. 2, the modulating and the carrier frequencies have been selected to be 98 Hz and 996 Hz, respectively. Thus, the LSB and USB frequencies are at 898 Hz and 1094 Hz, respectively.

Although both the DSB wave in Fig. 1(c) and the AM wave in Fig. 2(c) have similar envelopes, there are important differences between them. The AM wave displays a single wavepacket for each cycle of the modulating waveform, i.e., its envelope varies at the modulation frequency f_m, whereas the DSB wave displays two such wavepackets for each cycle of the modulating wave; its envelope varies at twice the modulation frequency $2f_m$. There are also subtle differences in the symmetry of the wavepackets since the AM modulating signal is always positive (it is a cosine wave shifted up in amplitude by unity) whereas the DSB modulating tone takes on both positive and negative values.

Demodulation of an analog AM signal

An AM signal passed through a nonlinear system is demodulated. The demodulated components include the modulation frequency and its harmonics (Schwartz, 1980). An essential requirement for demodulation is a transfer characteristic that is asymmetric for the positive and negative half-cycles of the modulated wave. The nonlinearity displayed by the stereocilia bundles of the hair cells when they are deflected results in asymmetric receptor potentials (Flock, 1965; Hudspeth and Corey, 1977). This nonlinearity will demodulate an AM sound by its asymmetric transfer function, and the resulting hair-cell receptor potential will contain the modulating signal. If the amplitude of the upper- and LSBs of the AM sound are not equal, the output will contain harmonics of the modulating signal as well as the modulating signal itself (Cuccia, 1952). This latter condition is frequently encountered in our nerve-fiber experiments.

Methods

The methods used in carrying out the experiments reported here are identical to those discussed previously and in the companion paper on FM signals (Teich and Khanna, 1985; Khanna and Teich, 1989), except as indicated below.

In all of the series of experiments involving modulation, the electrical input to the acoustic transducer (Sokolich, 1977) was calibrated for sound-pressure-level determination. For AM

stimuli, each carrier frequency f_c was amplitude modulated by a sinusoidal wave. The modulation frequencies used were $f_m = 20$, 40, 80, 160, 320 and 640 Hz. In most experiments 100% modulation depth was used. The carrier level was initially set at the threshold level of the FTC. Measurements were then carried out at the CF using the lowest modulation frequency (20 Hz). In successive measurements, the carrier level was increased in 10 dB steps to a maximum of 80 dB SPL. The measurements were repeated using the higher modulation frequencies. The entire series of measurements was then repeated using two or three additional carrier frequencies which, in the case of modulated tones, were chosen to be below and above the CF.

Period histograms were constructed from the nerve-spike data (Teich and Khanna, 1985). In Figs. 3–9(f), the histograms consisted of 4096 bins, each of 50 μs duration, so that one pass across the PST histogram represented 204.8 ms. In each of these figures, data were collected for 30 s, corresponding to about 150 repetitions. Thus, for a modulation frequency of 100 Hz, the period histogram contained about 20 modulation cycles. Since there was about 1 spike per modulation cycle on the average, there were a total of about 3000 spikes per histogram. The value of the spectral magnitude at DC, which represents the total number of spikes in the histogram, is therefore $\approx$ 3000 in these figures. For the data presented in Figs. 9(g)–14, on the other hand, the histograms consisted of 2048 bins, each 25 μs wide, representing a total duration of 51.2 ms per pass. In these figures, each histogram consisted of 100 repetitions over a total time of 5.12 s. The sounds were generated by the computer and the precise values of carrier and modulation frequencies were determined in accordance with the number of bins and the bin duration. Selecting a frequency of 100 Hz, for example, led to an actual frequency of 97.6 Hz (which we call 98 Hz). Thus the modulation and carrier frequencies were always commensurate and phase-locked with each other and with the averaging process.

Following the averaging, a discrete Fourier transform (DFT) of the histogram was constructed. The data reported in this paper are based on such DFT's.

Results

Full spectrum of the period histogram in response to DSB signals

In Fig. 3, the spectrum is shown for a unit with a CF of 2299 Hz and a threshold of 10 dB SPL. The DSB signal was centered at 996 Hz with a level at approximately 50 dB SPL. The DSB signal was generated by multiplying two cosine waves of equal amplitudes and frequencies 996 Hz and 98 Hz. Its spectrum consisted of a LSB at $f_1 = f_c - f_m = 898$ Hz and an USB of the same amplitude at $f_2 = f_c + f_m = 1094$ Hz. The difference frequency $f_2 - f_1$ was therefore 195 Hz (Fig. 1).

Nine components observed in the FFT of the histogram (Fig. 3) are: DC; $f_1 = 898$ Hz; $f_2 = 1094$ Hz; $2f_1 = 1796$ Hz; $2f_2 = 2188$ Hz; $f_2 - f_1 = 195$ Hz; $2f_1 - f_2 = 702$ Hz; $2f_2 - f_1 = 1290$ Hz; and $f_2 + f_1 = 1992$ Hz.

The response of the same unit at 50 dB SPL with $f_1 = 801$ Hz and $f_2 = 1191$ Hz is shown in Fig. 4. The eight strongest components appear at: DC; $f_1 = 801$ Hz; $f_2 = 1191$ Hz; $2f_2 = 2382$ Hz; $2f_1 - f_2 = 411$ Hz; $f_2 + f_1 = 1992$ Hz; $f_2 + 2f_1 = 2793$ Hz; and $2f_2 + f_1 = 3183$ Hz. With $f_1 = 606$

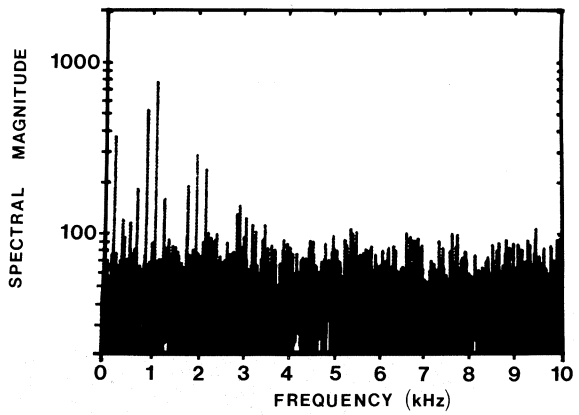

Fig. 3. Spectrum of the PST histogram in response to a DSB signal (CF = 2299 Hz, threshold $\approx$ 10 dB SPL) Spectral magnitude is displayed as a function of frequency. The input signal has a lower-sideband at $f_1 = 898$ Hz, an upper-sideband of the same amplitude at $f_2 = 1094$ Hz, and a level of about 50 dB SPL. This signal is illustrated in Fig. 1. Nine Fourier components of the spectrum clearly emerge above the noise. These are at: DC; $f_1 = 898$ Hz; $f_2 = 1094$ Hz; $2f_1 = 1796$ Hz; $2f_2 = 2188$ Hz; $f_2 - f_1 = 195$ Hz; $2f_1 - f_2 = 702$ Hz; $2f_2 - f_1 = 1290$ Hz; and $f_2 + f_1 = 1992$ Hz.

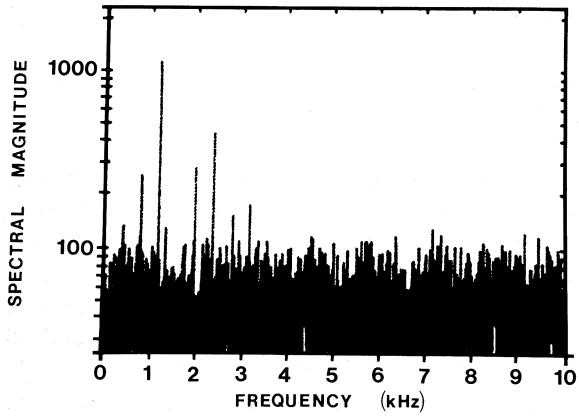

Fig. 4. Spectrum of the PST histogram for the same unit presented in Fig. 3. The signal level was maintained at 50 dB SPL but f_1 and f_2 were changed to 801 and 1191 Hz, respectively. In this case, eight Fourier components of the spectrum are clearly seen above the noise. These are at: DC; $f_1 = 801$ Hz; $f_2 = 1191$ Hz; $2f_2 = 2382$ Hz; $2f_1 - f_2 = 411$ Hz; $f_2 + f_1 = 1992$ Hz; $f_2 + 2f_1 = 2793$ Hz; and $2f_2 + f_1 = 3183$ Hz.

Hz and $f_2 = 1387$ Hz (Fig. 5), the nine strongest components are: DC; $f_1 = 606$ Hz; $f_2 = 1387$ Hz; $2f_2 = 2774$ Hz; $3f_2 = 4161$ Hz; $f_2 - f_1 = 781$ Hz; $2f_2 - f_1 = 2168$ Hz; $f_2 + f_1 = 1993$ Hz; and $2f_2 + f_1 = 3380$ Hz.

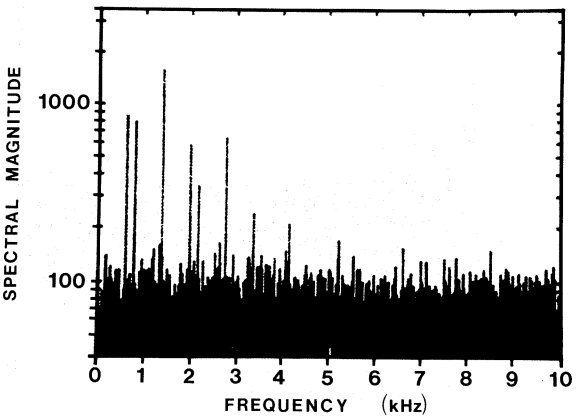

Fig. 5. Spectrum of the PST histogram for the same unit presented in Figs. 3 and 4. The signal level was maintained at 50 dB SPL but f_1 and f_2 were changed to 606 and 1387 Hz, respectively. Nine Fourier components of the spectrum are seen above the noise. These are at: DC; $f_1 = 606$ Hz; $f_2 = 1387$ Hz; $2f_2 = 2774$ Hz; $3f_2 = 4161$ Hz; $f_2 - f_1 = 781$ Hz; $2f_2 - f_1 = 2168$ Hz; $f_2 + f_1 = 1993$ Hz; and $2f_2 + f_1 = 3380$ Hz.

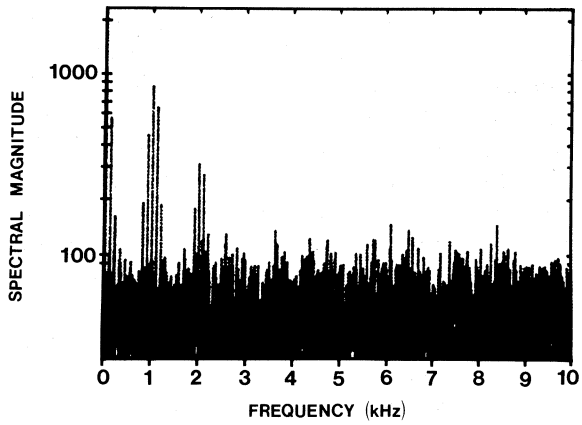

Fig. 6. Spectrum of the PST histogram in response to an AM signal for the same unit studied in Figs. 3–5 above (CF = 2299 Hz, threshold $\approx$ 10 dB SPL) The carrier frequency f_c was 996 Hz, the modulation frequency f_m was 98 Hz, and the level was $\approx$ 50 dB SPL. The input spectrum consisted of a component at the carrier frequency $f_c = 996$ Hz, a lower-sideband at $f_c - f_m = 898$ Hz, and an upper-sideband at $f_c + f_m = 1094$ Hz. The modulation depth was 100% so that the amplitudes of the sidebands were half that of the carrier. The signal for this experiment is illustrated in Fig. 2. The response consists of three clusters of spectral components that emerge above the noise floor. The leftmost cluster represents baseband components, which appear at DC and at the first five multiples of $f_m = 98$ Hz. The spectral components in the middle group are centered about the carrier frequency $f_c = 996$ Hz, and are spaced from it by $\pm f_m$ and $\pm 2f_m$. Finally, there is a cluster centered at twice the carrier frequency ($2f_c = 1992$ Hz).

Full spectrum of the period histogram in response to AM signals

Response below CF

The carrier frequency f_c was 996 Hz, the modulation frequency f_m was 98 Hz, the modulation depth was 100%, and the level was 50 dB SPL. Its spectrum consisted of components at 898 Hz, 996 Hz, and 1094 Hz (Fig. 2). The amplitudes of the sidebands were half that of the carrier. The spectrum of the period histogram for the same unit (CF = 2299 Hz, threshold $\approx$ 10 dB SPL) is presented in Fig. 6. It consists of three clusters of spectral components. The components in the lowest frequency cluster appear at DC and at the first five multiples of the modulation frequency (98 Hz). The next higher frequency cluster is centered about the carrier frequency (996 Hz). The spectral components are spaced from the carrier

by ± 98 Hz and ± 196 Hz. The magnitudes of the two sidebands nearest the carrier are unequal. The magnitude of the sideband at 898 Hz has about half the value of the component at f_c, whereas the sideband at 1094 Hz has a value of about three-quarters. The highest frequency cluster is centered around twice the carrier frequency (1992 Hz). The asymmetry of the spectral magnitudes in this third group parallels that of second group (centered at the carrier frequency). The magnitude of the clusters generally decreases with increasing frequency.

A comparison of the AM data in Fig. 6 with the DSB data in Fig. 2 shows some important differences. The separation of all the spectral components in the AM case is at the modulation frequency $f_m = 98$ Hz while in the DSB case the components are separated by twice the modulation frequency $2f_m = 195$ Hz. This difference is connected with the factor of 2 difference in the wavepacket-envelope frequencies shown in Figs. 1(c) and 2(c). A more subtle distinction relates to the spectral components at the carrier frequency and its harmonics. The carrier frequency (996 Hz) appears only in the AM case, as might be expected. However, in both cases a component appears at twice the carrier frequency (1992 Hz). It is present in AM because $2f_c = 1992$ Hz, but it is present in DSB because $f_2 + f_1 = 2f_c = 1992$ Hz.

Response at CF

The carrier frequency of the signal was increased to 2299 Hz. The input spectrum therefore consists of a component at the carrier frequency $f_c = 2299$ Hz, a LSB at $f_c - f_m = 2201$ Hz, and an USB at $f_c + f_m = 2397$ Hz.

The full spectrum of the period histogram shown in Fig. 7 for the same unit resembles that in Fig. 6. It consists of three clusters of components. Baseband components appear at the modulating frequency and its second harmonic. The spectral components of the middle group are centered around the carrier frequency (2299 Hz), and are spaced from it by $\pm f_m$ and $\pm 2f_m$. The magnitudes of the two sidebands ($f_c \pm f_m$) are approximately two-fifths as large as the carrier. The highest-frequency cluster is centered around twice the carrier frequency (4598 Hz), with sidebands

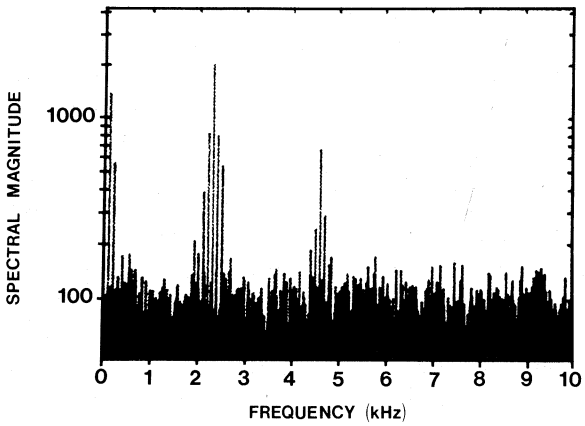

Fig. 7. Spectrum of the PST histogram for the same unit presented in Figs. 3–6. The conditions were identical to those indicated in Fig. 6 except that the carrier frequency of the signal was increased to $f_c = 2299$ Hz. The input spectrum therefore consists of a component at the carrier frequency $f_c = 2299$ Hz, a lower-sideband at $f_c - f_m = 2201$ Hz, and an upper sideband at $f_c + f_m = 2397$ Hz. The response consists of three clusters of spectral components that are seen above the noise floor: baseband components at the modulation frequency and its harmonics, components centered about the carrier frequency, and components centered about twice the carrier frequency.

separated from it by $\pm f_m$ and $\pm 2f_m$. The magnitudes of the components in a cluster decrease with increasing frequency of the cluster.

Response above CF

The pattern is repeated when the carrier frequency is increased to 2500 Hz (Fig. 8). The clusters of components appear at the baseband (three harmonics), around the carrier frequency (eight sidebands), and surrounding twice the carrier frequency (four sidebands). There is considerable asymmetry in the magnitude of the first LSBs and USBs ($f_c \pm f_m$). The LSB is about three times greater than the USB. The same is true for the sidebands at frequencies $2f_c \pm f_m$. The exaggeration of the LSBs is also observed for FM stimulation at a carrier frequency above the CF of the unit (Khanna and Teich, 1989; Fig. 6). The asymmetry in these sidebands is in the opposite direction to that observed for the response below CF. The magnitude of the component at the modulation frequency exceeds that of any of the sidebands.

General observations

It is apparent that the response spectrum resembles the acoustic waveform spectrum most closely when f_c is close to the CF; in this case the sidebands are approximately equal in magnitude (Fig. 7). When f_c differs from the CF, the sidebands exhibit asymmetries. The same is true for FM stimuli (Khanna and Teich, 1989; Fig. 5).

Although our results bear some similarity to those obtained by Javel (1980) in the chinchilla, there are substantive differences in our observations and interpretations. Javel recorded several different period histograms and examined his results principally in the time domain, whereas we examine ours in the frequency domain by using a single PST based on multiple periods of the complex tone. One important distinction is that for strong stimuli we see multiple baseband components whether or not the CF of a unit is tuned to these. Javel calls these intermodulation distortion products and attributed the presence of such components to the fact that the CF of the unit was tuned to the modulation frequency.

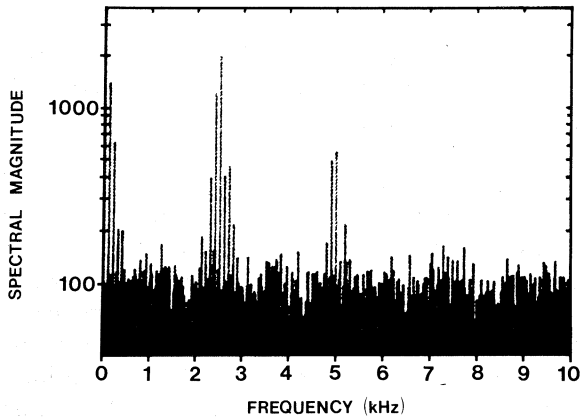

Fig. 8. Spectrum of the PST histogram for the same unit presented in Figs. 3–7. The conditions were identical to those indicated in Figs. 6 and 7 except that the carrier frequency of the signal is now increased to $f_c = 2500$ Hz. The input spectrum then consists of a component at the carrier frequency $f_c = 2500$ Hz, a lower-sideband at $f_c - f_m = 2402$ Hz, and an upper sideband at $f_c + f_m = 2598$ Hz. The pattern of three clusters in the response spectrum is repeated here: baseband components at the modulation frequency and its harmonics (three harmonics are visible), components centered about the carrier frequency (eight sidebands are visible), and components centered about twice the carrier frequency (four sidebands are visible).

Behavior of the baseband spectral components in response to AM signals for low-CF units

Definition of the baseband synchrony index (BSI)

The components in the lowest-frequency cluster occur at the modulation frequency and its harmonics. Because these low-frequency components may be of considerable significance in characterizing communication sounds, it is useful to study their normalized strength. We define the baseband synchrony index (BSI) as the ratio of the spectral magnitude at the fundamental modulation frequency to the spectral magnitude at DC.

This definition is analogous to the synchronization index (SI) which represents the ratio of the spectral magnitude at the carrier frequency to the spectral magnitude at DC (Anderson, 1973; Goldberg and Brown, 1969; Johnson, 1980). A value of 1.0 for the BSI indicates maximal synchrony, and a value of 0 minimal synchrony, of firing with the modulation frequency.

In analogy with the BSI, the nth-order baseband synchrony index, BSI(n), may be defined as the ratio of the spectral magnitude at the nth harmonic of the modulation frequency to the spectral magnitude at DC.

Variation of the baseband spectral magnitudes with depth of modulation

The baseband synchrony index (BSI) for the modulation frequency and its harmonics is shown in Fig. 9(a)–(c). The stimulus was at the CF (1597 Hz), at a level of approximately 40 dB SPL, and the modulation frequency was 19.5 Hz. The modulation depth M was 25% in (a), 50% in (b), and 100% in (c). The BSI increased in direct proportion to M, and the harmonics of the modulation frequency became more pronounced.

Variation of the baseband spectral magnitudes with signal level

The BSI for the modulation frequency and its harmonics is shown in Fig. 9(d)–(f). The stimulus was at the CF (3095 Hz), and the modulation frequency was 19.5 Hz. M was fixed at 100% and the stimulus level (dB SPL) was 20 dB in (d), 40 dB in (e), and 60 dB in (f). The BSI is seen to decrease with increasing stimulus level; however

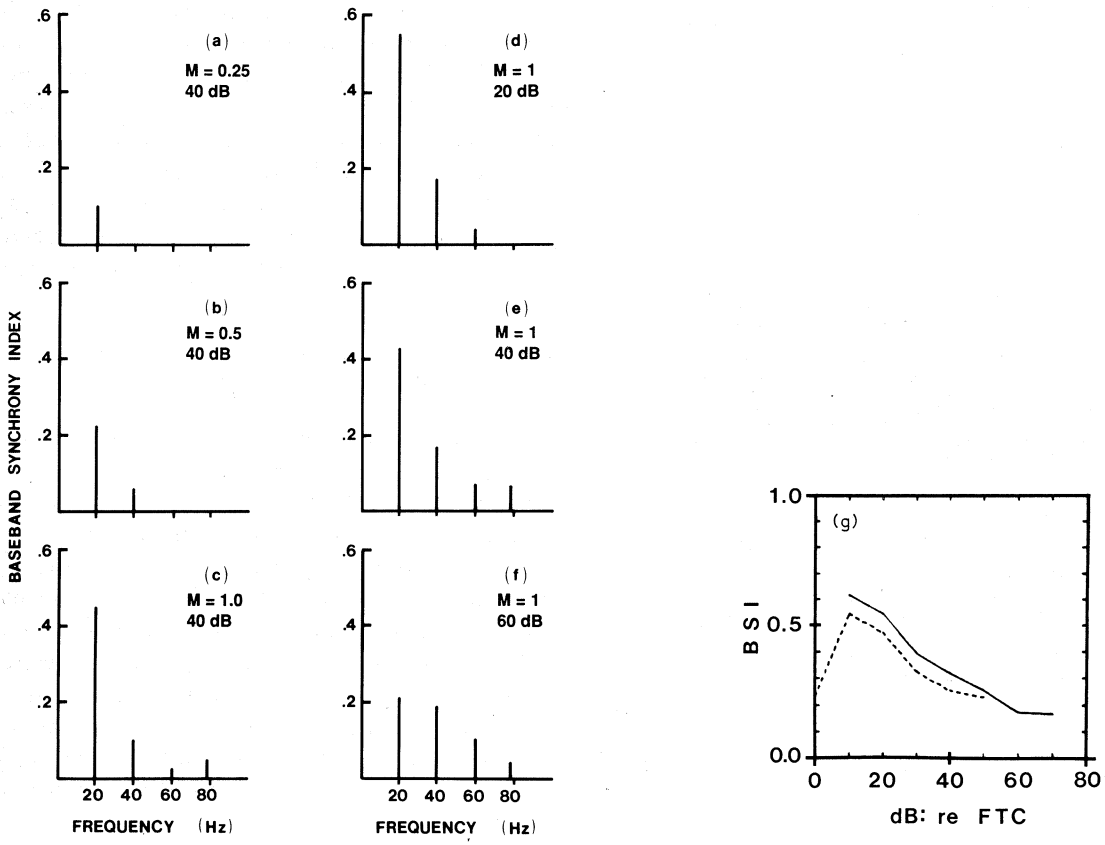

Fig. 9. (a)–(c) Baseband synchrony index (BSI) for the modulation frequency and its harmonics (CF = 1597 Hz) The BSI is defined as the ratio of the spectral magnitude at the modulation frequency, or its harmonics, to the spectral magnitude at DC (see text) The stimulus was at the CF, at a level of approximately 40 dB SPL, and the modulation frequency was 19.5 Hz. The modulation depth M is 25% in (a), 50% in (b), and 100% in (c) The BSI increases in direct proportion to M. Note that the harmonics of the modulation frequency become more pronounced as the modulation depth increases. (d)–(f) BSI for the modulation frequency and its harmonics (CF = 3095 Hz) The stimulus was at the CF, and the modulation frequency was 19.5 Hz. The modulation depth was 100% and the stimulus level (dB SPL) was varied: (d) 20 dB; (e) 40 dB; and (f) 60 dB. The BSI is seen to decrease with increasing stimulus level; however the magnitudes of the harmonics of the modulation frequency increase with stimulus level. (g) BSI as a function of signal level (CF = 1347 Hz) In this case the signal level is referred to the FTC threshold rather than to SPL (0 dB is then the FTC threshold) The carrier was at the CF (solid curve) and at 1074 Hz below the CF (dotted curve). The modulation frequency was 39 Hz and the modulation depth was 100%. The BSI magnitude reaches a maximum value at 20 dB:re FTC for both carrier frequencies even though the absolute stimulus levels for the two carrier frequencies differ by some 15 dB. This is because the FTC threshold is used as a reference. This suggests that the shape of the BSI curve may be independent of carrier frequency when FTC threshold is used as a reference.

the magnitudes of the harmonics of the modulation frequency increase with stimulus level.

The BSI for the modulation frequency is shown as a function of signal level in Fig. 9(g). In this case the signal level is referred to the FTC threshold. The carrier was at the CF (1347 Hz, solid curve) or below the CF (1074 Hz, dotted curve). The modulation frequency was 39 Hz and the modulation depth was 100%. It is interesting to note that the BSI magnitude reached a maximum value at 10 dB:re FTC for both carrier frequencies even though the absolute stimulus levels for the two carrier frequencies differed by some 15 dB. The baseband synchrony index, when plotted against stimulus level re FTC threshold, takes on a shape that is essentially independent of the carrier frequency. It begins to grow at about 10 dB below the FTC threshold and reaches its

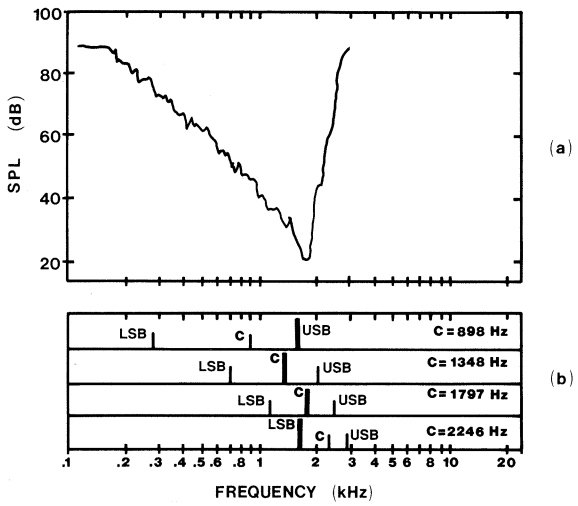

Fig. 10. (a) Frequency tuning curve for a unit with a CF of 1797 Hz and threshold of 20 dB SPL. (b) Frequencies of the spectral components at the carrier frequency (C), lower-sideband (LSB), and upper-sideband (USB) for four applied frequencies: 898 Hz, 1348 Hz, 1797 Hz, and 2246 Hz. The modulation frequency was 624 Hz. The component closest to the unit CF has been marked with a heavy line because it elicits the largest spectral response.

maximum value between 10 and 20 dB above the FTC threshold.

Behavior of the spectral components near the carrier frequency in response to AM signals

The FTC for a unit with a CF of 1797 Hz and a threshold of 20 dB SPL is shown in Fig. 10(a). In order to keep the spectral components well separated, the modulation frequency used was 624 Hz. Figure 10(b) displays the carrier frequency (C), LSB and USB for each of the four carrier frequencies used. The strongest spectral components have been marked with heavy lines. They occur at USB, C, C, and LSB, respectively, in the four successive panels. These are the components lying closest to the CF of the unit. This is a general property of the spectrum of the period histogram produced in response to amplitude-modulated signals: the component closest to the unit CF elicits the largest spectral response.

The dependence of the spectral magnitudes on sound pressure level are shown at four carrier frequencies, 898 Hz, 1348 Hz, 1797 Hz, and 2246 Hz, in Figs. 11(a), (b), (c), and (d), respectively. The spectral magnitudes of the carrier (C), LSB, USB, modulation frequency (BB), and DC are illustrated. The magnitude of each of these components is level dependent. Most of the components increase initially with signal level, reach a maximum, and then decline. In some cases, there is a second increase beyond the decline. It is also apparent that the rate-intensity function depends on the relationship between carrier frequency and CF.

Behavior of the baseband spectral components in response to AM signals for high-CF units

Variation of the baseband spectral magnitudes with signal level for a carrier at CF

The applied AM signal has a carrier frequency of 12988 Hz, a modulation frequency of 78 Hz, and a modulation depth of 100%. The spectral magnitude of the DC and baseband components as a function of stimulus level for a unit with a CF of 12988 Hz is shown in Fig. 12(a). Spectral components at the carrier frequency and its sidebands are near the noise floor because of loss of phase-locking. High-frequency units do not carry significant temporal information at the carrier or its sidebands.

On the other hand, the baseband component is clearly strong and dominant, reaching its maximum value at relatively low stimulus levels, slowly decreasing at higher stimulus levels, but remaining a significant component even at the highest SPLs. Thus high-frequency units carry information at the modulation frequency of an AM signal. This is illustrated more clearly by the baseband synchrony index, which is displayed as a function of signal level in Fig. 12(b). The BSI is 0.65 at the lowest stimulus levels shown, decreasing to 0.1 at the highest stimulus levels. Since the input AM signals do not contain baseband components, it is clear that their presence in the output spectrum reveals an internal demodulation process.

Dependence of the baseband spectral magnitudes on carrier frequency

The carrier frequencies used were: (a) 10488 Hz (below CF); (b) 12988 Hz (at CF); and (c) 14492 Hz (above CF). The two modulation frequencies used were: 39 Hz (solid curves) and 624 Hz (dashed curves).

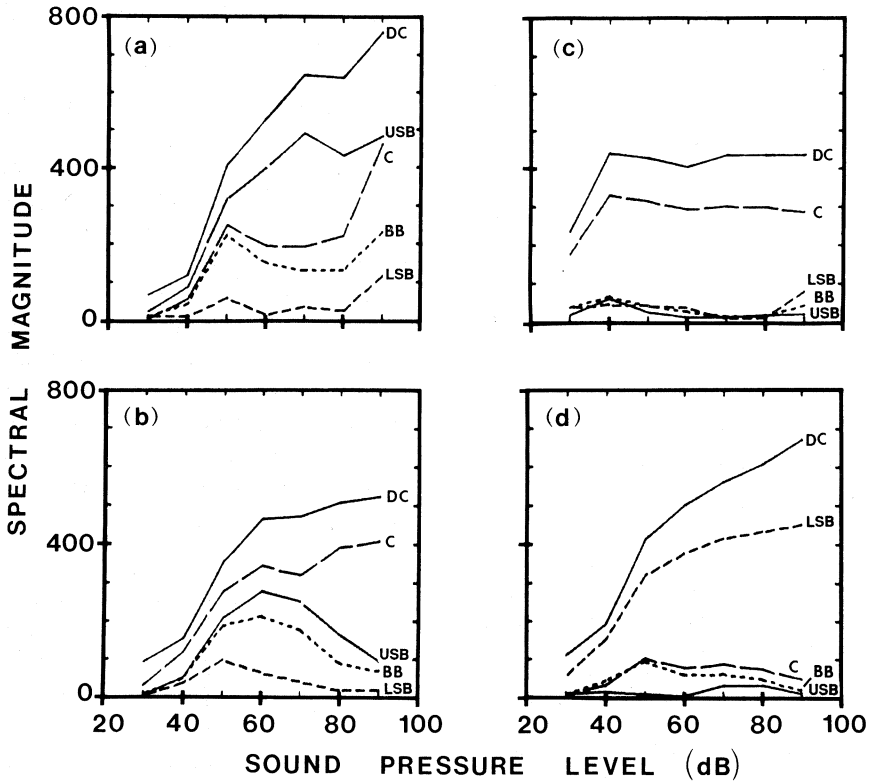

Fig. 11. Spectral magnitudes of the carrier (C), lower-sideband (LSB), upper-sideband (USB), modulation frequency (baseband BB), and DC as a function of stimulus level for the unit shown in Fig. 10. Carrier frequencies used were: (a) $f_c = 898$ Hz; (b) $f_c = 1348$ Hz; (c) $f_c = 1797$ Hz; (d) $f_c = 2246$ Hz. The magnitude of each of these components is level dependent. Many components initially increase with signal level, reach a maximum, and then decline. In some cases, there is a second increase beyond the decline.

The baseband spectral magnitude versus stimulus level curves shown in Fig. 13 are similar in shape for the two modulation frequencies, at each of the three carrier frequencies. However, the shapes of the baseband spectral magnitude curves are different. When the carrier frequency is below CF, the spectral magnitude increases with stimulus level, reaching a maximum at about 70 dB SPL, and remaining essentially flat to 90 dB (Fig. 13(a)). With the carrier at CF, the spectral magnitude has already reached a maximum value at 40 dB SPL, and decreases slowly as the stimulus level is increased to 90 dB SPL (Fig. 13(b)). Finally, when the carrier is above CF, the spectral magnitude generally increases with stimulus level, reaching a maximum value at approximately 60 dB (Fig. 13(c)). Above 70 dB the magnitude decreases slowly.

Dependence of the baseband spectral magnitudes on modulation frequency

The baseband spectral magnitude versus modulation frequency for this same unit is shown in Fig. 14 for modulation frequencies of 40, 80, 160, 320, and 640 Hz and carrier frequencies of (a) 10488 Hz (below CF); (b) 12988 Hz (at CF); and (c) 14492 Hz (above CF). Results are shown for four stimulus levels (30, 50, 70, and 90 dB SPL).

At each of the carrier frequencies, the baseband spectral magnitude is approximately independent of modulation frequency; i.e., the responses are essentially flat for each of the signal levels.

Discussion

For DSB signals, spectral components in the nerve-spike train were found at frequencies given

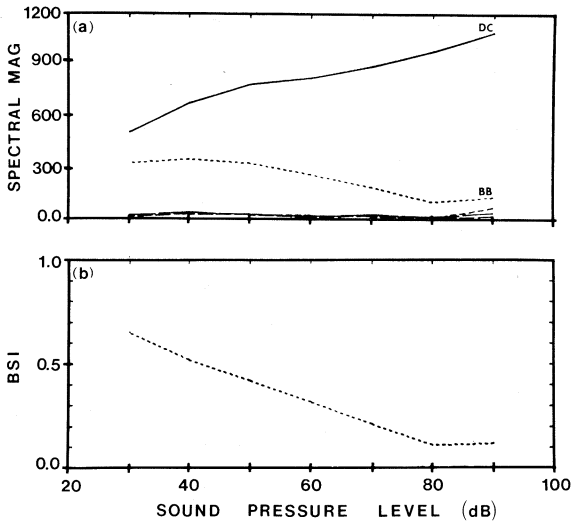

Fig. 12. (a) Spectral magnitude of DC and baseband components as a function of stimulus level (CF = 12988 Hz) The applied AM signal has a carrier frequency $f_c = 12988$ Hz, a modulation frequency $f_m = 78$ Hz, and a modulation depth of 100%. Components at the carrier frequency and its sidebands, near the noise floor, are also shown. The baseband component is clearly strong and dominant, reaching its maximum value at relatively low stimulus levels. Its magnitude decreases at higher stimulus levels. (b) The baseband synchrony index is displayed as a function of signal level. The BSI is 0.65 at 30 dB SPL and decreases to 0.1 at 90 dB SPL

by

$$f_{DSB} = jf_2 \pm k(f_2 - f_1),\ j = 0,1,2,...;\ k = 0,1,2,... . \quad (2)$$

When the difference frequency $f_2 - f_1$ is small, these components form spectral clusters. For large values of $f_2 - f_1$, however, the various spectral component clusters overlap and interdigitate (Teich and Khanna, 1989). Since only the lower and USB frequencies (f_1 and f_2, respectively) are contained in the input auditory signal, the other components seen in the response are produced by a nonlinear transduction process internal to the ear.

Clusters of spectral components were also present in the nerve-spike train in response to AM signals of carrier frequency f_c and modulation frequency f_m. The frequencies of the components are given by the sequence

$$f_{AM} = jf_c \pm kf_m,\ j = 0,1,2,...;\ k = 0,1,2,... . \quad (3)$$

The lowest-frequency cluster has components at DC, at the modulation frequency, and at its harmonics. These components were strong and were found to be present for all fibers studied, whatever their CF. The next group contains spectral components centered at the carrier frequency and at frequencies separated from it by the modulation frequency and its harmonics. Higher-frequency clusters are centered around multiples of the carrier frequency and at frequencies separated from these multiples by the modulation frequencies and its harmonics.

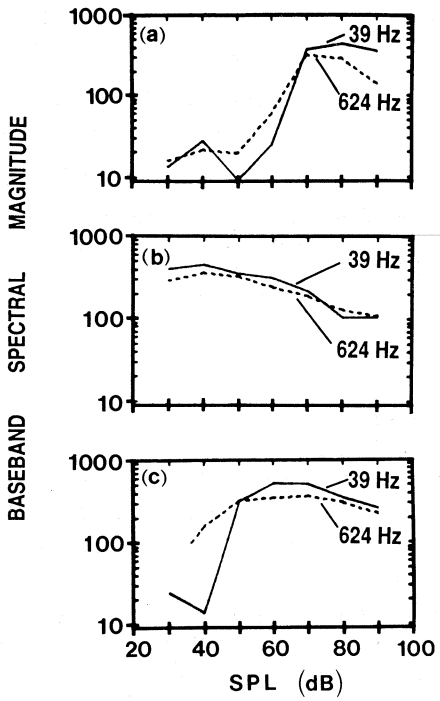

Fig. 13. Baseband spectral magnitude as a function of stimulus level for the same unit shown in Fig. 12. Data are shown for three carrier frequencies: (a) $f_c = 10488$ Hz (below CF); (b) $f_c = 12988$ Hz (at CF); and (c) $f_c = 14492$ Hz (above CF) Results for two modulation frequencies are shown: $f_m = 39$ Hz (solid curves) and $f_m = 624$ Hz (dashed curves) The baseband spectral magnitude reaches a maximum at different values of the stimulus intensity when the carrier frequency is below CF, at CF, and above CF. This level is lowest when the carrier is at the CF

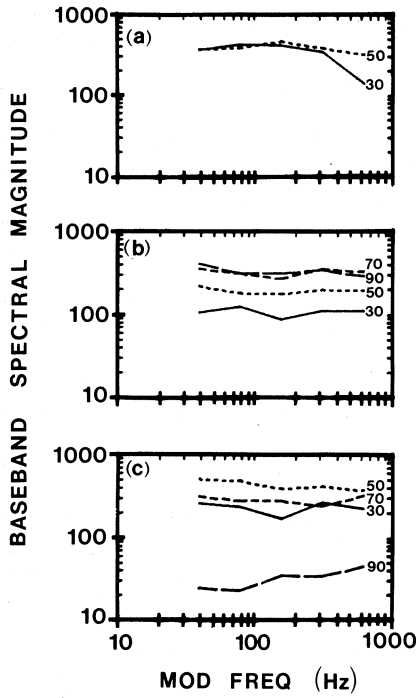

Fig. 14. Baseband spectral magnitude as a function of modulation frequency for the same unit shown in Figs. 12 and 13. Modulation frequencies used were $f_m = 40$, 80, 160, 320, and 640 Hz. The carrier frequencies of the applied AM signal were: (a) $f_c = 10488$ Hz (below CF); (b) $f_c = 12988$ Hz (at CF); and (c) $f_c = 14492$ Hz (above CF) Results for four stimulus levels (30, 50, 70, and 90 dB SPL) are shown. The baseband spectral magnitude is approximately independent of modulation frequency for each carrier frequency and stimulus level

The relative spectral magnitudes of the carrier, and its LSBs and USBs, are dependent on their frequencies with respect to the tuning curve of the unit. Components located at, or near, the CF of the unit are emphasized whereas those located away from the CF are deemphasized. The degree of attenuation is dependent on the shape of the tuning curve (the wider it is the less the attenuation) and on the frequency separation of the sidebands from the carrier (the lower the modulation frequency the less the attenuation).

The relative magnitudes of the carrier, sideband, and baseband spectral components depend on the CF of the unit. For CFs below about 1 kHz (for carrier frequencies at the CF with 100% modulation depth), the carrier magnitude is higher than the sideband magnitudes, and the baseband magnitude is comparable with the sideband magnitudes. The carrier and sideband magnitudes decrease for CFs above 1 kHz. Between 2 and 3 kHz the carrier and sideband magnitudes become smaller than the baseband magnitude. Above 5 kHz, the carrier and sideband magnitudes become negligibly small although the baseband spectral magnitude remains large. Therefore, even though high-frequency nerve fibers do not carry high-frequency temporal information (Johnson, 1980) they carry information efficiently at the modulation frequency.

The baseband signal therefore provides an important means of carrying information in low- and medium-CF fibers and the exclusive means of carrying such information in high-CF fibers. Because of the importance of the baseband components, we have defined a normalized index for their strength. The baseband synchrony index (BSI) is the ratio of the spectral magnitude at the fundamental modulation frequency to the spectral magnitude at DC. We have found BSI values as high as 0.9 for low-CF units and 0.7 for high-CF units. Such large values for the BSI indicate that the nerve-spike firings of primary auditory fibers are well synchronized with the applied modulation frequency for the amplitude-modulated signals we have considered. This, in turn, means that the fiber is carrying information contained in the envelope of the signal. A number of other observations indicate the importance of the baseband signal: (i) it appears at low signal levels close to the neural threshold; (ii) its magnitude is appreciable over a broad range of stimulus levels; (iii) its magnitude remains constant over a wide range of modulation frequencies; and (iv) its magnitude is approximately proportional to the modulation depth. These observations suggest an AM demodulation process in the inner ear, and an efficient neural coding system for the transmission of modulated signals.

A nerve-spike train evoked in response to a modulated signal, when passed through a low-pass filter (with a cutoff frequency comparable to the modulation frequency), produces the modulation frequency at the output (Khanna and Teich, 1989). The nerve-spike train normally undergoes just such low-pass filtering in transmission through a synaptic junction. Intracellular potentials recorded from the postsynaptic cell should therefore con-

tain the modulation signal. The extraction of the baseband signal from the nerve-spike train is therefore achieved with the natural functioning of the system. The experiments reported here, and in the companion paper on FM signals (Khanna and Teich, 1989), are consistent with the interpretation that the auditory system acts principally to detect modulation rather than pure tones (Teich and Khanna, 1989). The auditory nonlinearity is an essential component of this demodulation process. The ability of the auditory system to demodulate AM and FM signals may be highly significant for speech recognition.

The information in the nervous system is transmitted by means of nerve spikes and is therefore digital in nature. Our experiments with modulated signals suggest that at each cellular level the incoming digital nerve spike train is low-pass filtered to produce an analog modulation signal and its harmonics. The analog signals generated by multiple synaptic inputs to a given cell are integrated, in analog form, and the resulting signal is utilized to initiate a new output nerve spike train encoding the integrated analog signal. Thus it appears that the process of neural transmission is digital in nature whereas the processing itself is analog.

Acknowledgments

We are grateful to David Lund and Robert O'Connor for contributions to software development. We thank James Kelly and Suzanne Keilson for editorial suggestions. Support was provided by the National Institutes of Health (NINCDS) and by the National Science Foundation through the Center for Telecommunications Research in the School of Engineering and Applied Science at Columbia University.

References

Abbas, P. J. and Sachs, M. B. (1976) Two-tone suppression in auditory-nerve fibers: Extension of a stimulus-response relationship. J. Acoust. Soc. Am. 59, 112–122.

Anderson, D.J. (1973) Quantitative model for the effects of stimulus frequency on synchronization of auditory nerve discharges. J. Acoust. Soc. Am. 54, 361–364.

Arthur, R. M., Pfeiffer, R. R. and Suga, N. (1971) Properties of 'two-tone inhibition' in primary auditory neurones. J. Physiol. 212, 593–609.

Britt, R. and Starr, A. (1976) Synaptic events and discharge patterns of cochlear nucleus cells. II. Frequency modulated tones. J. Neurophysiol. 39, 179–194.

Cuccia, C.L. (1952) Harmonics, Sidebands and Transients in Communication Engineering. McGraw-Hill Inc., New York.

de Ribaupierre, F., Goldstein, M. H., Jr.and Yeni-Komshian, G. (1970) Responses of single cortical cells to repetitive clicks. J. Acoust. Soc. Am. 48, 123.

Evans, E.F. (1978) Place and time coding of frequency in the peripheral auditory system: Some physiological pros and cons. Audiology 17, 369–420.

Evans, E.F.and Nelson, P.G. (1966) Responses of neurones in cat cochlear nucleus to modulated tonal stimuli. J. Acoust. Soc. Am. 40, 1275.

Fernald, R.D. and Gerstein, G.L. (1972) Response of cat cochlear nucleus neurons to frequency and amplitude-modulated tones. Brain Res. 45, 417–435.

Fletcher, H. (1953) Speech and Hearing. Van Nostrand, New York.

Flock, Å. (1965) Transducing mechanisms in the lateral line canal organ receptors. Pp 133–147, Cold Spring Harbor Symposia on Quantitative Biology, Vol. XXX. Cold Spring Harbor Laboratory of Quantitative Biology – Cold Spring Harbor, N.Y.

Galambos, R. and Davis, H. (1944) Inhibition of activity in single auditory nerve fibers by acoustic stimulation. J. Neurophysiol. 7, 289–303.

Glattke, T.J. (1969) Unit responses of the cat cochlear nucleus to amplitude-modulated stimuli. J. Acoust. Soc. Am. 45, 419–425.

Greenberg, S., Geisler, C. D. and Deng, L. (1986) Frequency selectivity of single cochlear-nerve fibers based on the temporal response pattern to two-tone signals. J. Acoust. Soc. Am. 79, 1010–1019.

Goldberg, J.M. and Brown, P.B. (1969) Response of binaural neurons of dog superior olivary complex to dichotic tonal stimuli: Some physiological mechanisms of sound localization. J. Neurophysiol. 32, 613–636.

Greenwood, D.D. (1986) What is synchrony suppression? J. Acoust. Soc. Am. 79, 1857–1872.

Greenwood, D.D. (1988) Cochlear nonlinearity and gain control as determinants of the response of primary auditory neurons to harmonic complexes. Hear. Res. 32, 207–253.

Horst, J.W., Javel, E. and Farley, G.R. (1985) Extraction and enhancement of spectral structure by the cochlea. J. Acoust. Soc. Am. 78, 1898–1901.

Horst, J.W., Javel, E. and Farley, G.R. (1986) Coding of spectral fine structure in the auditory nerve. I. Fourier analysis of period and interspike interval histograms. J. Acoust. Soc. Am. 79, 398–416.

Hudspeth, A.J. and Corey, D.P. (1977) Sensitivity, polarity and conductance change in the response of vertebrate hair cells to controlled mechanical stimuli. Proc. Natl. Acad. Sci. USA, 74(6), 2407–2411.

Javel, E. (1980) Coding of AM tones in the chinchilla auditory nerve: Implications for the pitch of complex tones. J. Acoust. Soc. Am. 68, 133–146.

Javel, E. (1981) Suppression of auditory nerve responses I: Temporal analysis, intensity effects and suppression contours. J. Acoust. Soc. Am. 69, 1735–1745.

Javel, E., Geisler, C. D. and Ravindran, A. (1978) Two-tone suppression in auditory nerve of the cat: Rate-intensity and temporal analyses. J. Acoust. Soc. Am. 63, 1093–1104.

Johnson, D.H. (1980) The relationship between spike rate and synchrony in response of auditory-nerve fibers to single tones. J. Acoust. Soc. Am. 68, 1115–1122.

Khanna, S.M. and Teich, M.C. (1989) Spectral characteristics of the responses of primary auditory-nerve fibers to frequency-modulated signals. Hear. Res. 39, 159–176.

Littlefield, W. M. (1973) Investigation of the linear-range of the peripheral auditory system. Sc. D. thesis, Washington University (Available from University Microfilms, Ann Arbor, MI, No. 74–13808)

Møller, A.R. (1971) Unit responses in the rat cochlear nucleus to tones of rapidly varying frequency and amplitude. Acta Physiol. Scand. 81, 540–556.

Møller, A.R. (1972a) Coding of amplitude and frequency modulated sounds in the cochlear nucleus of the rat. Acta Physiol. Scand. 86, 223–238.

Møller, A.R. (1972b) Coding of sounds in lower levels of the auditory system. Quart. Rev. Biophys. 5, 59–155.

Møller, A.R. (1973) Coding of amplitude-modulated sounds in the cochlear nucleus of the rat. In: Basic Mechanisms in Hearing. A.R. Møller (Ed.), Academic Press, New York, pp. 593–617.

Møller, A.R. (1974) Responses of units in the cochlear nucleus to sinusoidally amplitude-modulated tones. Exp. Neurol. 45, 104–117.

Møller, A.R. (1976) Dynamic properties of primary auditory fibers compared with cells in the cochlear nucleus. Acta Physiol. Scand. 98, 157–167.

Nelson, P. G., Erulkar, S. D. and Bryan, J. S. (1966) Responses of units of the inferior colliculus to time-varying acoustic stimuli. J. Neurophysiol. 29, 834–860.

Rose, J.E., Brugge, J.F., Anderson, D.J. and Hind, J.E. (1968) Patterns of activity in single auditory nerve fibers of the squirrel monkey. In: Hearing Mechanisms in Vertebrates. A.V.S. deReuck and J. Knight (Eds.), Little Brown, Boston. pp. 144–157.

Sachs, M. B. and Kiang, N. Y-S. (1968) Two-tone inhibition in auditory-nerve fibers. J. Acoust. Soc. Am. 43, 1120–1128.

Schwartz, M. (1980) Information Transmission, Modulation, and Noise. McGraw Hill, New York.

Sinex, D.G. and Geisler, C.D. (1981) Auditory-nerve fiber responses to frequency-modulated tones. Hear. Res. 4, 127–148.

Smith, R.L. and Brachman, M.L. (1980) Response modulation of auditory-nerve fibers by AM stimuli: Effects of average intensity. Hear. Res. 2, 123–133.

Sokolich, W. G. (1977) Improved acoustic system for auditory research. J. Acoust. Soc. Am. (Suppl. 1) 62, S12.

Teich, M.C. and Khanna, S.M. (1985) Pulse-number distribution for the neural spike train in the cat's auditory nerve. J. Acoust. Soc. Am. 77, 1110–1128.

Teich, M.C. and Khanna, S.M. (1989) Spectral encoding of acoustic signals in primary auditory-nerve fibers: Theory, in prep.

Vartanian, I. A. (1971) Impulse activity of neurons of the rat's inferior colliculus in responses to amplitude-modulated sound signals. In: Sensory Processes at the Neuronal and Behavioral Levels. G. V. Gersuni (Ed.), Academic, New York, pp. 201–220.